Neuron
Article

Associative Cortex Features in the First Olfactory Brain Relay Station

Wilder Doucette,[1,2,5] David H. Gire,[1,2,5] Jennifer Whitesell,[2,3] Vanessa Carmean,[2,3] Mary T. Lucero,[4] and Diego Restrepo[1,2,*]
[1]Department of Cell and Developmental Biology
[2]Neuroscience Program
[3]Department of Physiology and Biophysics
University of Colorado Anschutz Medical Campus, Aurora, CO 80045, USA
[4]Department of Physiology, University of Utah, Salt Lake City, UT 84112, USA
[5]These authors contributed equally to this work
*Correspondence: diego.restrepo@ucdenver.edu
DOI 10.1016/j.neuron.2011.02.024

SUMMARY

Synchronized firing of mitral cells (MCs) in the olfactory bulb (OB) has been hypothesized to help bind information together in olfactory cortex (OC). In this survey of synchronized firing by suspected MCs in awake, behaving vertebrates, we find the surprising result that synchronized firing conveys information on odor value ("Is it rewarded?") rather than odor identity ("What is the odor?"). We observed that as mice learned to discriminate between odors, synchronous firing responses to the rewarded and unrewarded odors became divergent. Furthermore, adrenergic blockage decreases the magnitude of odor divergence of synchronous trains, suggesting that MCs contribute to decision-making through adrenergic-modulated synchronized firing. Thus, in the olfactory system information on stimulus reward is found in MCs one synapse away from the sensory neuron.

INTRODUCTION

In invertebrates associative learning resulting in adequate responses to stimuli is mediated partially by plasticity in the synapse that the sensory neuron makes with a second-order neuron (Bailey and Kandel, 2008; Roberts and Glanzman, 2003). However, in vertebrates synaptic changes that encode for the value associated with a stimulus take place several synapses downstream from the sensory neuron (Gold and Shadlen, 2007; Komura et al., 2001; Pantoja et al., 2007). Potential exceptions are in V1 cortex in the visual system (Shuler and Bear, 2006), the brainstem in the gustatory system (Chang and Scott, 1984), and within the olfactory system, where learning-induced changes occur within the olfactory bulb (OB) one or two synapses away from the sensory neuron (Friedrich et al., 2004; Gao and Strowbridge, 2009; Gray et al., 1986; Kay and Laurent, 1999; Nissant et al., 2009; Wilson and Leon, 1988). However, it is not clear whether learning-related plasticity in these early circuits represents a modulation in the circuitry to enhance discrimination or whether it plays a more dynamic role and actively contributes to the encoding of stimulus value (Kay and Laurent, 1999). Please note that when we refer to odor value, we do not exclude the possibility that the circuit may carry information on a related reward signal (Wallis and Kennerley, 2010).

Olfactory sensory neurons transform information about the chemical structure of an odor into neuronal activity and transmit information synaptically to second-order cells, including the mitral cells (MCs) (Shepherd et al., 2004; Tan et al., 2010). Interneuron circuits within the OB modulate MC firing and likely provide contrast enhancement (Aungst et al., 2003; Mori et al., 1999; Shepherd et al., 2004), and learning modifies activity of MCs through plasticity that is likely caused by feedback from neuromodulatory systems and centrifugal input from the olfactory cortex (OC) back into the OB (Doucette and Restrepo, 2008; Gao and Strowbridge, 2009; Mandairon and Linster, 2009; Restrepo et al., 2009; Wilson and Mainen, 2006). Interestingly, studies of odor-induced oscillatory field potentials in olfactory discrimination tasks suggest the involvement of changes in synchronous firing between neurons in the OB circuit in learning in vertebrates (Gray et al., 1986; Kay and Beshel, 2010; Martin et al., 2006). In addition, MCs are hypothesized to aid in synthesis of simultaneously detected odor features through synchronized firing and convergence on neurons in OC (Kashiwadani et al., 1999; Mori et al., 1999), which has been supported by experiments in invertebrates (Stopfer et al., 1997). Studies in vertebrates are consistent with the claim that synchronous firing of MCs increases the probability of driving target OC neurons (Franks and Isaacson, 2006; Luna and Schoppa, 2008). However, direct evidence for synchronized firing of MCs in vertebrates is limited to a measurement of synchrony in anesthetized animals (Kashiwadani et al., 1999) that was not replicated (Egaña et al., 2005). Thus, the precise role of synchronized MC firing in transfer of olfactory information, in learning of olfactory stimulus/reward association, or in both is not well understood.

Here we measure synchronized spiking in suspected MCs (SMCs; see Experimental Procedures) in awake, behaving mice engaged in a go-no go behavioral task wherein they learn to recognize a new odor as rewarded. We ask whether

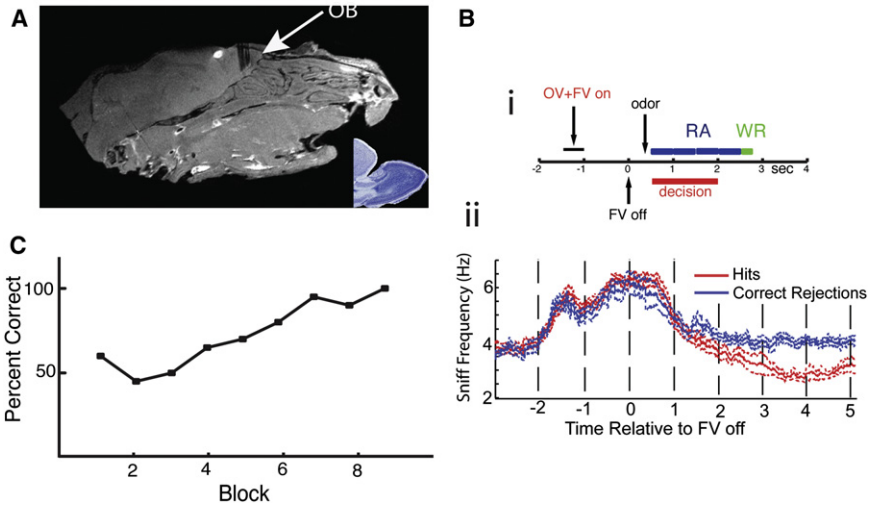

Figure 1. Overview of Odor Discrimination Task

(A) Sagittal MRI of the mouse's head showing the location of the electrodes. The inset is a Nissil stained sagittal section of an adult mouse's OB.

(Bi) Time course for trials in the odor discrimination task (Slotnick and Restrepo, 2005). When the mouse inserts its head into the odor chamber, an odor valve (OV) opens, directing the odor into the air stream, and simultaneously a final valve (FV) opens, directing the air stream to exhaust ("OV+FV on"). At time zero FV turns off ("FV off"), eliciting an abrupt odor onset at approximately 0.3 s measured with a photoionization detector (PID) (see Experimental Procedures). The animal must lick for the rewarded odor on the water delivery tube at least once for four 0.5 s periods (blue blocks) in the response area (RA). The red bar shows the range of decision times (Doucette and Restrepo, 2008). If the animal licks correctly, it receives water during a Water Reward (WR) period.

(Bii) Sniffing behavior during the odor discrimination task. Mice increase sniff frequency in anticipation of odor presentation, and decrease sniff frequency steadily during odor presentation. As the decision is made, sniff frequency is reduced to basal levels for correct rejections and below basal levels following the water reward for hits (rewarded trials) (11 sessions across five animals, significant difference starting at 1.68 s after FV off, ranksum test, $p < 0.05$). Data is displayed as mean ± SEM.

(C) Percent correct responses as a function of the block number (20 trials per block, 10 rewarded and 10 unrewarded). The mice learn to refrain from licking to the unrewarded odor.

synchronized firing conveys information on odor identity ("What is the odor?"), or alternatively, value ("Is it rewarded?"). In addition, noradrenergic (NA) modulation is known to play a role in new olfactory stimulus/reward association (Bouret and Sara, 2004; Doucette et al., 2007), and we ask whether NA antagonist application in the OB affects synchronized spike odor responses of SMCs to rewarded and unrewarded odors in the go-no go behavioral task. We find that responses of synchronized SMC spikes to odors convey information on odor value (or a related reward signal), and that the differential synchronized spike response to rewarded and unrewarded odor is not as robust in the presence of inhibitors of NA modulation of the OB. Thus, the olfactory system stands out from other sensory systems in that information on stimulus value is found in the MC that is one synapse away from the sensory neuron, in the same place in the circuit as would be a bipolar cell in the visual system or a spiral ganglion cell in the auditory system.

RESULTS

Go-No Go Task

Mice were implanted with two eight-microelectrode arrays targeted to the MC layer (Figure 1A). During each trial in the go-no go task, thirsty mice were asked to respond to a rewarded odor by licking a tube, and they received a water reward if they licked at least once in the last four 0.5 s periods of the trial (the response area [RA]; see Figure 1Bi; no reward for the unrewarded odor). The sniffing behavior of animals during this task is illustrated in Figure 1Bii. Consistent with previous reports (Wesson et al., 2008), animals showed an increase in sniffing frequency in anticipation of odor presentation. Sniffing frequency started differing between successful rewarded and unrewarded odor trials at ~1.7 s in the middle of the decision-making period, when mice steadily reduced their breathing rates to a final frequency of 2–3 Hz after the water reward. Figure 1C shows an example of how a mouse learns to respond in a session wherein the animal is presented with a new pair of odors. Mice stop responding to the unrewarded odor because the licking entails considerable effort that is not rewarded with water. Mice learned to respond reliably (more than 80% correct) within 3–6 blocks of 20 trials (10 rewarded and 10 unrewarded) (Slotnick and Restrepo, 2005).

Precise Synchronization between Spikes from Different SMCs

We recorded from 345 single units and 820 multiunits in the MC layer of eight animals in 67 separate sessions (39 first day and 28 reversals). In recordings from mice performing odor discrimination, we find precise synchronization between a subset of spikes (Figure 2). Figure 2A shows precise spiking for three SMCs, and Figures 2B1 and 2B2 show the histograms of interspike lags. As in Doucette and Restrepo (2008), spikes were identified as voltage deviations greater than three times the standard deviation (SD) of the noise in extracellular voltage recordings. Single-unit spikes were separated from all other spikes using unsupervised spike sorting (see Experimental Procedures). Multiunits were all spikes left after identification of single-unit spikes, and spike time was defined as the time of the peak of the voltage deviation. As shown in the histograms in Figures 2B1–2B3, synchronization is precise, with spikes from different units firing within <250 μs (in the Supplemental Text available online, we rule out artifactual spike pairing). Precise synchronous firing was also found when a single unit was compared to a multiunit (Figure 2B3) and when multiunits were compared to each other (not shown). Hereafter we define synchronized spikes as spikes that happen within less than 250 μs.

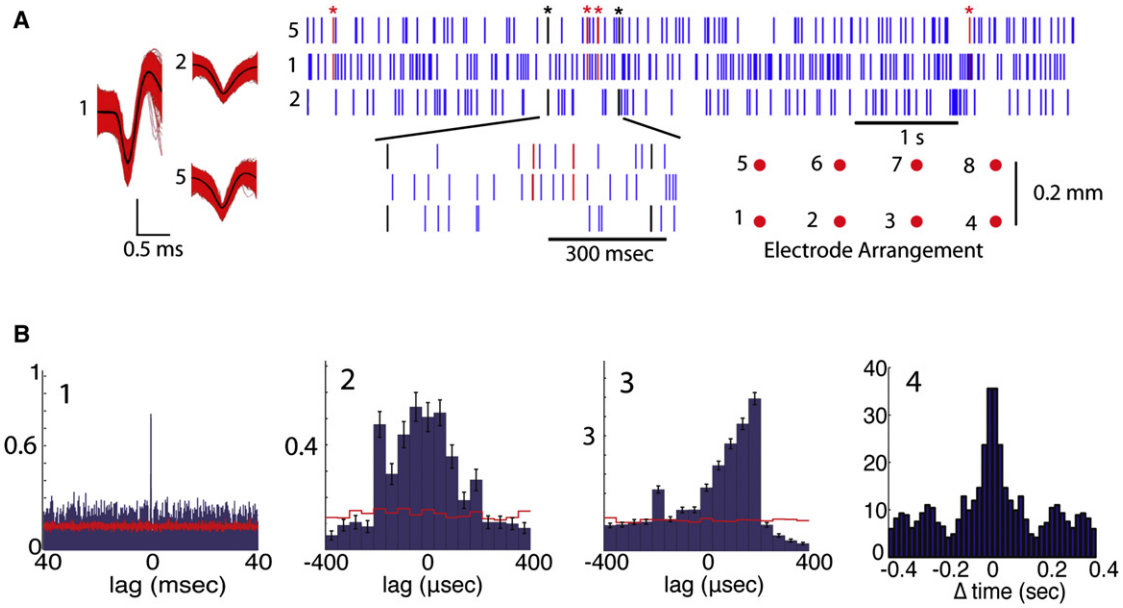

Figure 2. Precise Synchronized Firing between SMCs

(A) Scatterplots for three single units recorded from electrodes 5, 1, and 2 (spike shapes shown on left with a vertical scale bar of 0.5 mV and microelectrode layout shown on lower right). Spikes synchronized within <250 μs between units 5 and 1: red (asterisk); between 5 and 2: black (asterisk).

(B1–B3) Lag histograms. The y axis shows the number of spikes per trial in the reference unit that lag by the time delay denoted by each bin when compared with spikes in the partner unit. (B1 and B2) For the units in channels 5 and 1, 1.8% of spikes are synchronized. (B3) Histogram for one single unit and a multiunit (6.4% synchronized spikes). Red lines are lag histograms calculated after spikes were shuffled randomly ± 1 mean ISI.

(B4) Average autocorrelogram for the synchronized spike trains (from 2857 multiunit pairs in the RA). An autocorrelogram calculated after shifting the reference unit spikes by a random time within ± 1 ISI was subtracted from the data and the result was normalized by dividing by the shifted autocorrelogram. The number of animals in this study is 8, the number of units recorded from was 345 (SU) and 820 (MU), and the number of pairs recorded from was 578 SU×SU, 1620 MU×SU and SU×MU, and 4391 MU×MU. Recording was performed in 67 sessions (39 first day and 28 reversals).

The average fraction of synchronized spikes was significantly different from the fraction of synchronized spikes arising by chance (compare red line to histograms in Figures 2B1–2B3, and see Experimental Procedures) and ranged from 0.9% for single-unit pairs (SU×SU, n = 138) to 6.0% for multiunit pairs (MU×MU, n = 2578; see Table 1). As shown in Figure 2A, synchronized spikes were sparse in single-unit pairs. Sparseness in these SU×SU synchronized trains made it difficult to calculate statistics for changes in firing rate elicited by odors. Therefore when evaluating odor-induced changes we used synchronized trains estimated from multiunit pairs. Importantly, in the Supplemental Text and in Figure S1 (available online), we show that the percent of synchronized spikes in MU×MU pairs is consistent with the makeup of the multiunit spikes by single units, and in Figure S2 we show that the waveforms of the synchronized multiunit spikes do not differ from those of the rest of the spikes in the multiunit. Finally, an autocorrelogram of the synchronized spike trains in the RA shows a weak oscillatory pattern (at ~5 Hz, Figure 2B4) consistent with changes in simultaneous synchronized firing associated with breathing.

Synchronized Spike Trains Develop a Divergent Odor Response

Figure 3Ai shows the development of differential responsiveness to new odors by synchronized spike trains through a go-no go session. As shown in an earlier study for spikes from individual units (Doucette and Restrepo, 2008), in the first 20-trial block, the synchronized spike trains do not respond differentially to the two odors (Figures 3Ai and 3B), and the mouse does not respond differentially to the odors (Figure 3C). In contrast, after 60–100 trials (three to five blocks), the animal develops a differential behavioral response and the synchronized spike trains respond with excitation to the rewarded odor, and with inhibition

Table 1. Percentage of Spikes Synchronized in a Unit Pair

Unit Pairs: Reference Unit × Partner Unit	Percentage of Spikes Synchronized: Mean ± SD (n)
SU×SU	0.9 ± 1.1 (138)
MU×SU	0.7 ± 1.1 (566)
SU×MU	3.7 ± 6.7 (566)
MU×MU	6.0 ± 6.1 (2578)

Unit pairs are classified depending upon whether the units were single units (SU) or multiunits (MU). The table shows the average percentage of spikes within the reference unit that are within 250 μs of one of the spikes in the partner unit (synchronized spikes). The percentage of synchronized spikes (%Synch) in the RA was calculated from the number of spikes in the reference unit (n_{ref}), the number of synchronized spikes (n_{synch}), and the number of synchronized spikes in the reference unit after ISI shuffling (n^{Sh}_{synch}): %Synch = $100(n_{synch} - n^{Sh}_{synch})/ n_{ref}$. This value is calculated for those unit pairs that are significantly synchronized in 39 sessions.

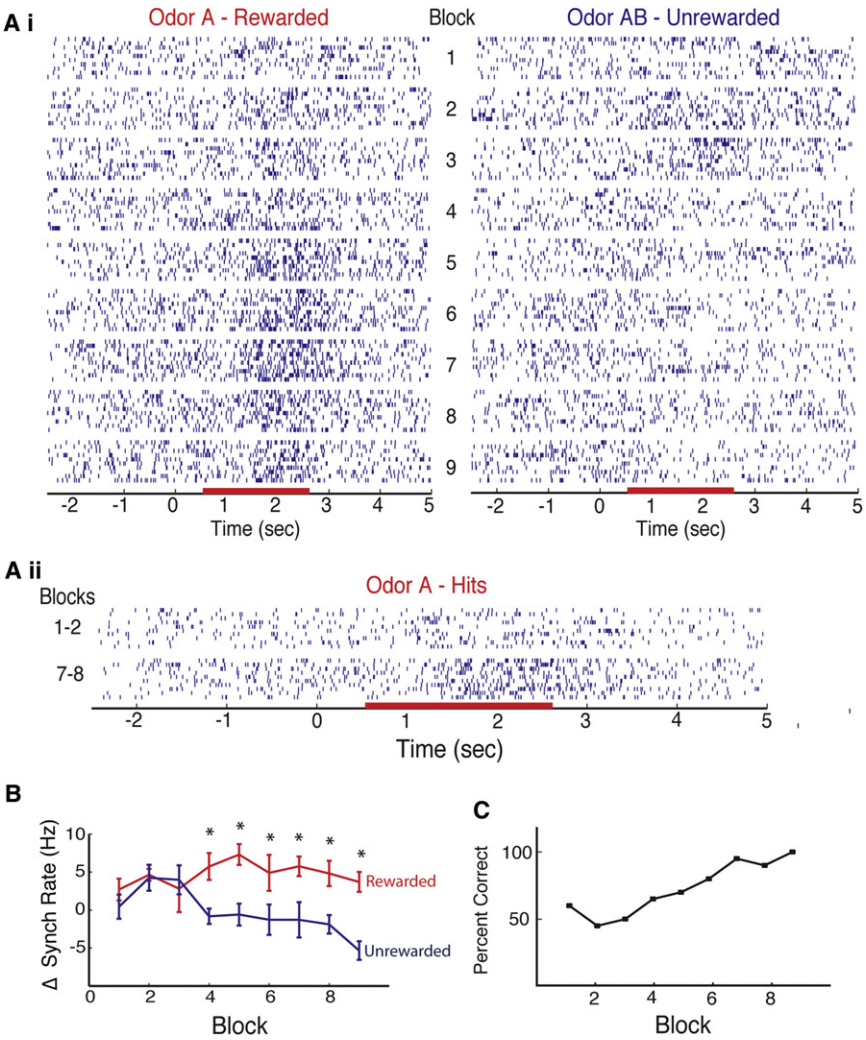

Figure 3. Example of Synchronized Firing in the Odor Discrimination Task

(Ai) Scatterplot for synchronized spike firing for all blocks in a session. Each block has 20 trials (10 rewarded and 10 unrewarded). As shown, the synchronized trains develop an excitatory response to the rewarded odor and an inhibitory response to the unrewarded odor.

(Aii) Side-by-side comparison of the synchronized spike firing in hit trials in blocks 1 and 2 and 7 and 8.

(B) Odor-induced change in rate of synchronized firing for the data in (A). Firing rate was calculated as the firing rate in the RA minus rate in the previous 2 s. Rewarded red and unrewarded blue, mean ± SEM, n = 10 trials (*$p < 0.05$, corrected for multiple comparisons by FDR).

(C) Behavioral percent correct responses for the same session.

to the unrewarded odor. Responses were classified as divergent using a t test corrected for multiple comparisons through false discovery rate (FDR) with a significant p value in at least two blocks in a session (see Experimental Procedures). The most divergent block (best block) varied from blocks 2 to 9 for synchronous firing in different multiunit pairs (mean is block 6 with SD of 2.4, n = 48 pairs). These data show that divergent responses of synchronized spike trains develop during learning.

Importantly, in the first two blocks wherein the animal is performing at chance (Figure 3C) when it licks correctly to the rewarded odor (a trial denoted as a "hit"), there is little change in synchronized firing over time (Figure 3Aii). In contrast, in later blocks (i.e., blocks 7 and 8), wherein the animal responds correctly in over 80% of the trials, there is a robust excitatory response to the odor in the hit trials (Figure 3Aii). Although the animal is performing the same action in hit trials for blocks 1 and 2 and blocks 7 and 8, the odor only induces synchronized train responses in the later blocks. Lack of responses in hit trials in blocks 1 and 2 indicates that the odor-induced increases in synchronized firing rate are not a result of common source noise caused by stereotyped movement during licking in the hit trials (see also Supplemental Text).

Responses of Synchronized Trains Are Either Excitatory or Inhibitory Depending on Whether the Odor Is Rewarded

Do synchronous spikes carry information unavailable in spike trains from individual units considered in isolation? Figure 4Aii shows the average z-score defined as the average odor-induced change in firing rate in a block of 20 trials divided by the SD before odor application. A z-score greater than zero indicates an increase in firing rate, whereas a z-score less than zero indicates a decrease in firing rate. The z-scores were derived from the block of trials that showed the largest odor-induced divergence in synchronous firing (solid lines) or in spike firing rates of each unit considered in isolation (broken lines). The average z-score curves for the units (all spikes, not just synchronous spikes; broken lines) show that when all spikes are counted without regard to synchrony, rewarded odor responses (red) could be either increases or decreases in firing rate, and that unrewarded odor responses (blue) had some increases, but were mostly decreases. In contrast, when only synchronous spikes were considered (solid lines), the odor responses were much more informative, because they were "divergent" in that the rewarded odor (red) always yielded an increase in synchronous firing, and the unrewarded odor (blue) always elicited a decrease in synchronous firing (Figure 4Aii, solid lines).

Synchronized Spikes Carry Information on Odor Reward

Do the synchronized spikes carry information on odor identity or odor reward? We addressed this question by reversing the

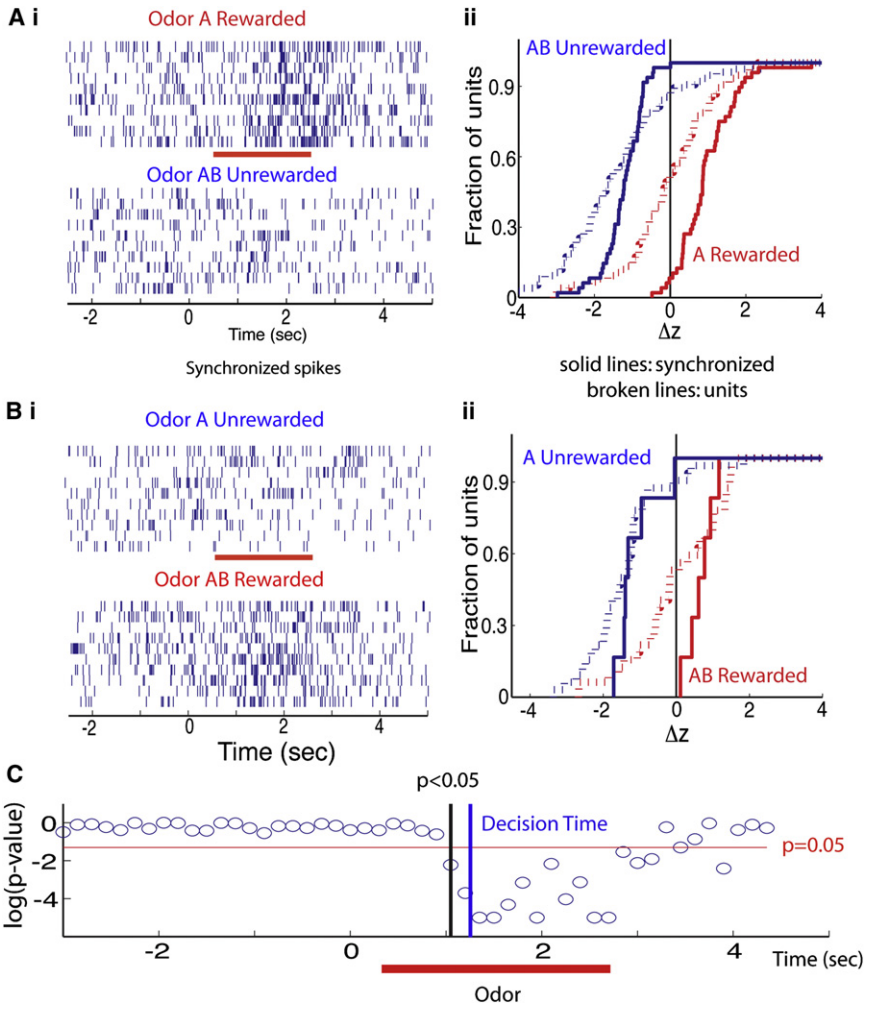

Figure 4. Odor Responses of Spikes Synchronized between Two Multiunits

Spike trains are shown for one block of the session wherein the mice learned to differentiate between odors A (rewarded) and AB (unrewarded) (Figure 4A) and one for a second session wherein the odors were reversed for reward (AB rewarded, A unrewarded) (Figure 4B). Synchronized spikes were those firing in both units within <250 μs, and the block chosen (the best block) was the one wherein the odor responses to the two odors were most divergent. (Ai) Synchronized spike trains for divergent odor responses in best block (trials: 10 rewarded, 10 unrewarded; red bar is the RA [0.5 to 2.5 s) for the rewarded odor). (Aii) Z-score cumulative histogram in best block for 68 spike trains for multiunit odor-divergent responses (broken lines) and for 48 odor-divergent synchronized spike trains. Z-score was calculated as the RA firing rate minus the rate for the 2 s preceding the RA divided by the SD of the rate in the preceding interval. The magnitude of the difference in z-score between rewarded and unrewarded odor did not correlate with the timing of when the best (most divergent) block occurred (correlation coefficient of 0.05, $p = 0.76$). Synchronized spike trains (Bi) and z-score cumulative histogram (Bii) for odor reversal session including 31 multiunits (broken lines) and 6 multiunit synchronized pairs (solid lines, $n = 6$) (odor A, blue-unrewarded; and odor AB, red-rewarded) are shown. (C) p value for a ranksum test reporting on the difference in the Euclidean distance between rewarded and unrewarded odor responses in principal component (PC) space. PC analysis was calculated for the time course of synchronized spike firing in multiunits in all trials within the best block (see Figure S3 for the results of the PC analysis). The response to the rewarded and unrewarded odors diverges at ~1 s. The animal makes a decision to stop licking for the unrewarded odor at ~1.25 s (blue line, determined by a ranksum test of the difference in licks in best blocks with >85% correct responses).

value of the odor. Comparing z-score cumulative histograms for the first session wherein odor A was rewarded and AB unrewarded (Figure 4Aii) with those in the reversal wherein AB was rewarded while A was unrewarded (Figure 4Bii) shows a remarkable effect of value reversal. Regardless of the identity of the odor, synchronized spike trains (solid lines in Figures 4Aii and Bii) displayed an increase in firing in response to the rewarded odor and a decrease in response to the unrewarded odor. Thus, the information conveyed by synchronous spikes is related to the odor's value rather than the odor's identity.

Synchronized Responses to the Two Odors Diverge before the Animal Makes a Decision

At this point we asked whether the information on the value of the odor conveyed by the synchronized firing trains diverged between the two odors at a time in the trial before the animal made a decision. We performed principal component (PC) analysis of divergent synchronized pair responses to the odors. Figure S3A shows, for the first and best blocks, the time course for the responses to odors in 2D PC space, and Figure S3B shows the time course of the Euclidean distance in PC space between the points for the rewarded and unrewarded odors. There is clear divergence of the responses to the odors in the best block, but not in the first block. Figure 4C shows the p value for a ranksum test of divergence of the Euclidean distance between rewarded and unrewarded odors. Divergence of synchronized unit firing becomes significant at ~1 s (0.7 s after addition of the odor), which is ~0.25 s earlier than the time at which the animals make a decision to stop licking to the unrewarded odor (1.25 s, estimated with a ranksum test on licks). A fraction of a second afterward at ~1.7 s, the mice change their sniff frequency (Figure 1Bii). Thus, the divergence between rewarded and unrewarded odors for synchronized trains carries information that the animal can use for odor discrimination.

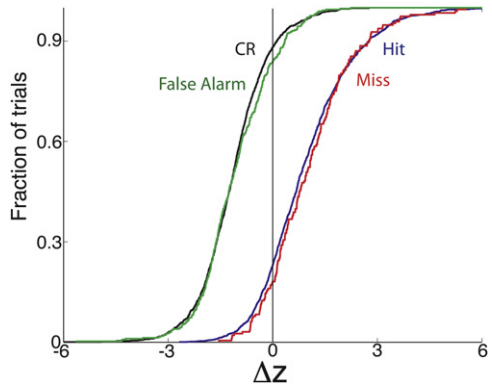

Figure 5. Cumulative Histograms of the Responses of Synchronized Firing of Pairs of Multiunits to Odors in the Odor Discrimination Task, Shown Separately for Trials Wherein the Animal Makes the Correct Behavioral Decision (Hits, Blue; and Correct Rejections [CR], Black) and for Trials Involving an Incorrect Decision (False Alarm, Green; and Miss, Red)

Responsiveness was calculated as a z-score defined in the Experimental Procedures on a trial-per-trial basis in divergent blocks that included at least one mistake. A positive z-score indicates that the synchronized firing rate increased upon exposure to the odor. An ANOVA with a post hoc test indicated that the z-scores for miss were not different from the z-scores for hits and that the responses from false alarms did not differ from those of correct rejections. There was a significant difference between hits/misses and correct rejections/false alarms. In order to ensure that the incorrect trials mirrored the correct trials, we also did an ANOVA wherein we only included false alarms, wherein the animal licks for 80% or more of the time in the 2 s RA, and misses, wherein the animal licked less than 20% of the time in the RA. The ANOVA test yielded the same differences/lack of differences between hits, misses, correct rejections, and false alarms. The number of trials included are as follows: 1431 hits, 193 misses, 1219 correct rejections, and 378 false alarms.

Synchronized Train Odor Responses in Trials Where the Animal Made a Mistake

We next asked whether analysis of trials where the animals made mistakes shows that synchrony reflected responses to odor, and not responses that mirrored the behavioral action. In other words, when the animal makes a mistake and licks on the water tube to obtain a reward when exposed to the unrewarded odor (false alarm), are the synchronized spike trains more like the synchronized firing that takes place when the animal correctly licks for a water reward to a rewarded odor (hit), or more like the synchronized responses when the animal correctly does not lick for the unrewarded odor (correct rejection)? As shown by the z-score cumulative histograms in Figure 5, the synchronized spiking decreased ($\Delta z < 0$) in response to the unrewarded odor, regardless of whether the animal licked during this odor (false alarm, green) or not (correct rejection, black). Similarly, for the majority of the trials, synchronized firing increased ($\Delta z > 0$) in response to the rewarded odor whether the animal licked during this odor (hit, blue) or refrained from licking (miss, red). Thus, the odor-induced changes in synchronized firing are responses to the odor as opposed to responses that follow the animal's behavior or licking. In addition, because the responses follow the odor presented rather than the movement the animal made, the data in this figure indicate that the synchronized spike trains are not brought about by noise caused by the animal's movements.

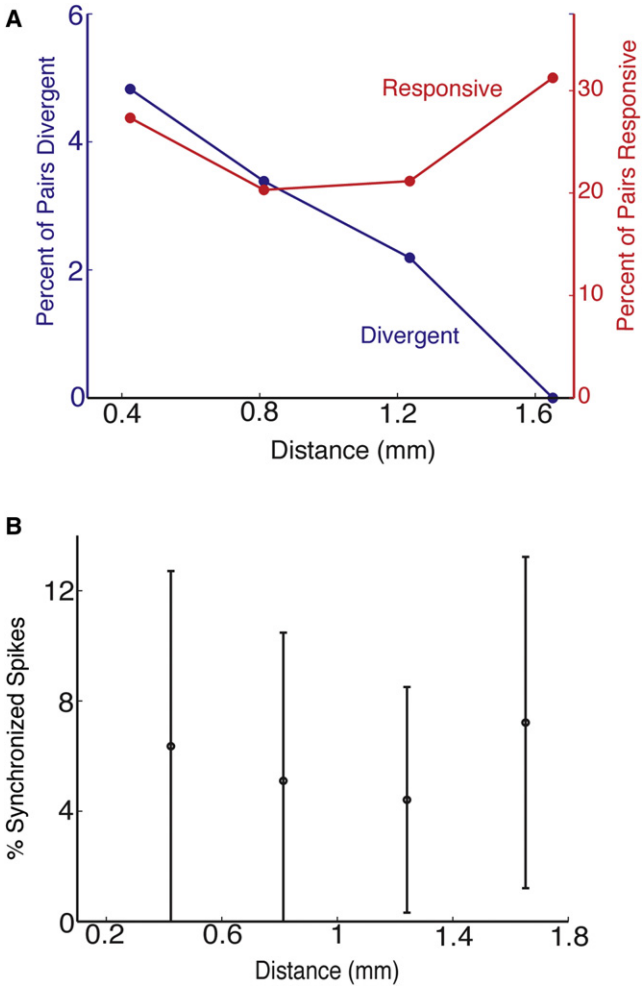

Figure 6. Distance Dependence

(A) Odor responsiveness of synchronized spike trains for unit pairs was recorded during the odor discrimination behavioral task (as in Figures 3 and 4). This panel shows, as a function of distance between recording electrodes, the percent of unit pairs whose synchronized spike trains were responsive to odors (red) and the percent of unit pairs whose synchronized spike trains were differentially responsive to the rewarded and unrewarded odors (blue). The number of pairs used to calculate percent values at each distance are (in order of ascending distance) 742, 380, 143, and 35.

(B) Percentage of synchronized spikes in a reference unit shown as a function of distance between the electrode recording the reference unit spike train and the electrode recording the partner unit spike train (only MU×MU pairs were included). The values shown are the mean of the percentage of spikes that are synchronized, plus or minus SD. The number of pairs used to calculate each point are (in order of ascending distance) 1498, 790, 280, and 64.

The Circuit Mediating Divergent Synchronized Spike Responses Is Limited in Spatial Extent

The percent of unit pairs whose synchronized spike trains respond differentially to the odors decreased as a function of distance between electrodes (Figure 6A, blue). Importantly, this decrease in the percent of unit pairs exhibiting divergent responses for synchronized spikes as a function of distance is in sharp contrast with the absence of a decrease in the percent

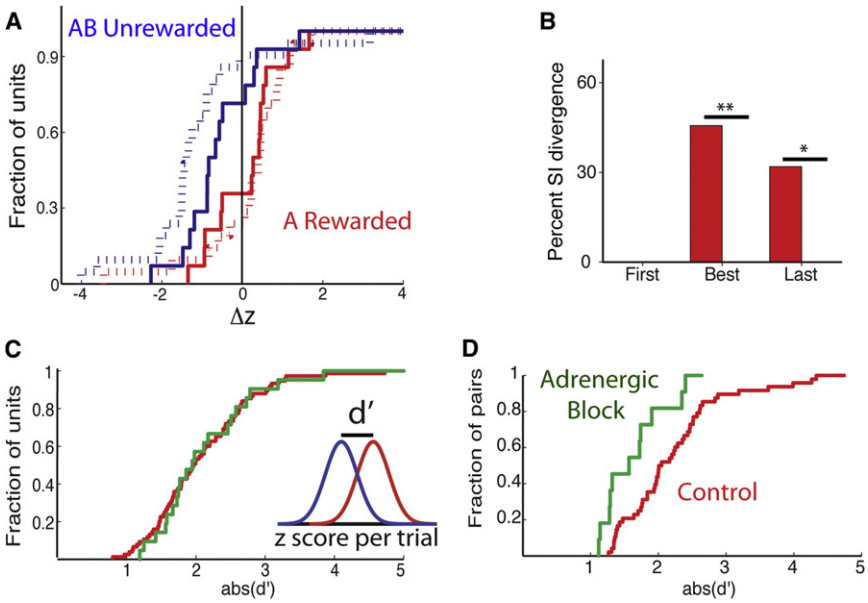

Figure 7. Adrenergic Blockade

(A) Z-score for 20 unit odor responses that were significantly divergent (broken lines) and for 14 odor-divergent synchronized pairs (solid lines) (red, rewarded; blue, unrewarded; calculated in the best block).

(B) Percentage of odor-divergent synchronized pairs with a significant difference in the percentage of synchronized spikes between rewarded trials and unrewarded trials. *p = 0.016, **p = 0.0016 (Chi-square test, n = 48 control, 14 adrenergic). The rest of the divergent synchronized pairs changed synchronized firing due solely to an increase in firing rate of the reference unit.

(C) d′ calculated as the difference in z-score between rewarded and unrewarded unit odor responses. The inset illustrates how d′ was calculated (red, control; green, adrenergic block).

(D) d′ for synchronized spike trains. The two histograms do not differ in (C) ($p > 0.05$ in K-S test), but do differ in (D) ($p = 0.01$). All synchronized pairs were from multiunits.

of synchronized spike trains responsive to odors as a function of distance (Figure 6A, red), and the absence of a change in the percent of synchronized spikes for each unit pair as a function of distance (Figure 6B). These data show that divergent responsiveness for synchronized firing is effective within a limited distance (<1.5 mm). In addition, the difference in dependence on electrode-to-electrode distance between divergence and responsiveness of synchronized firing of unit pairs indicates that synchronized firing is not due to synchronous electrode noise (see also Supplemental Text).

NA Modulation Participates in Conveying Information on Odor Reward through Synchronized Spikes

The data presented above show that synchronized spike SMC output is modified in a manner dependent on behavioral context (i.e., on whether the new odor is rewarded). This context-dependent modification is likely mediated by centrifugal innervation into the OB from olfactory cortical networks and/or neuromodulatory centers (Mandairon and Linster, 2009; Restrepo et al., 2009). Interestingly, blockade of adrenergic receptors in the OB prevents mice from discriminating closely related novel odors in the go-no go task (Doucette et al., 2007), and adrenergic activation results in enhanced synchronized oscillations of the local field potential in the bulb (Gire and Schoppa, 2008). These studies motivated us to ask whether blocking the adrenergic receptors in the OB affects differential synchronized spike odor responsiveness to rewarded and unrewarded odors. For adrenergic drug delivery animals received bilateral restricted injection into the OB of a solution with α and β adrenergic blockers under isoflourane anesthesia (Doucette et al., 2007) 10 min prior to the go-no go task. Application of the drugs resulted in delay of discrimination between odors in the go-no go task (Figure S4C).

Application of α and β adrenergic blockers diminished the magnitude of divergent synchronized spike train responses to odors in the go-no go task. Figure 7A shows the average z-scores for responses to odors (red, rewarded; blue, unrewarded). While the unit average z-score cumulative histograms are similar in the presence/absence of adrenergic block (compare broken lines in Figures 7A and 4Aii), the responses of synchronized spike trains appeared different compared with those of controls. Specifically, rewarded odors elicited some inhibitory responses in the presence of adrenergic blockers, but did not do so in controls (compare where solid red lines cross zero [vertical black line] in Figures 7A and 4Aii).

To quantify the magnitude of the difference in average z-scores between rewarded and unrewarded odor trials, we calculated the d′, the difference in z-score between the responses to the rewarded odors and those to the unrewarded odors (see inset in Figure 7C). Figure 7C shows that d′ for units did not differ between control (red) and adrenergic antagonist (green) conditions. In sharp contrast, adrenergic blockade elicited a clear left shift in d′ for synchronized spike trains, as would be expected for loss of magnitude of the divergence in z-scores (leftward shift in green [adrenergic] line compared to red [control] line in Figure 7D). Interestingly, and consistent with the left shift in d′, for odor-divergent pairs there was a sharp reduction in the odor-induced change in percent of synchronized spikes between adrenergic block and control (Figure 7B, also see Figure S4). Thus, the odor-induced changes in synchronized firing in the presence of adrenergic block are entirely due to changes in firing rate of the reference units, not changes in the percent of synchronized spikes.

DISCUSSION

Our findings indicate that the firing of synchronized spikes between groups of SMCs, the second-order neurons in the olfactory circuit, carries information on odor value or on other reward signals, such as attention and vigilance (Wallis and

Kennerley, 2010). An observer can make a decision on odor value based on whether the number of synchronized spikes fired by SMCs increases or decreases in response to an odor. Thus, placing a vertical line at $\Delta z = 0$ in Figure 4Aii allows successful discrimination between rewarded ($\Delta z > 0$) and unrewarded ($\Delta z < 0$) odor based on synchronized firing responses to odors (solid lines). In contrast, there is no vertical line that ensures successful determination of odor value based on the odor responses of the units that make up the synchronized firing pair (Figure 4Aii, broken lines). Interestingly, odors, like tastants, vary in whether they are naturally perceived as attractive or repulsive. Based upon this observation, we would predict that naturally repulsive odors would yield decreases in synchronized firing, whereas attractive odors would yield increases, with reversals as the animal is trained otherwise. The observed learning-induced plasticity in the OB that provides information on odor value could contribute to downstream plasticity, decision-making, or the estimation of expected outcomes used in prediction error calculations.

The precise timing for synchronization of spikes in different SMCs (spikes that lag by <250 μs; Figure 2) raises the question of whether this is due to common source noise from a biological action (e.g., grinding of teeth or licking). An advantage of using the go-no go task is that behavior is stereotyped for hit trials wherein the animal must lick during the RA. We asked whether biological actions during this stereotyped behavior in hit trials could have yielded the increase in synchronized firing observed during responses to the rewarded odor. After all, if all hit trials display high levels of synchrony (due, perhaps, to movements the animals make during licking), an increase in synchronized firing to the rewarded odor could appear as the session progresses simply because more hit trials are associated with the rewarded odor. In order to account for this possible confound, we compared the odor responsiveness of hit trial synchronized spiking during the first set of trials in the session (while the animal was responding randomly to the rewarded odor with many hits and misses) with hit trials later in the session when the animal was responding to the rewarded odor almost exclusively with hits (Figure 3Aii). There was no odor-induced increase in synchronized spike firing in the hit trials at the beginning of the session. This demonstrates that the observed increase in synchronized firing was not due to biological, common noise occurring consistently during hit trials. In addition, common noise artifacts tend to affect voltage recorded by multiple electrodes. The fact that synchronized spikes occur in different unit pairs exclusively (Figures 2A and S1, and Supplemental Text) is evidence that these are not due to common noise. Further, since divergence in synchronized firing is clearly dependent upon the distance between electrodes (Figure 6B, blue points), it is not plausible that biological, common source noise is the source of this synchronization, because biological, common noise occurring across units should not depend on the distance between electrodes. Finally, if the synchronized spikes were common noise, their shape would be expected to differ from that of the unsynchronized spikes, and this is not the case (Figure S2). These observations and other findings (see Results and Supplemental Text) show that the precisely synchronized spikes are not due to common noise.

The precise timing for synchronization of spikes in different SMCs (spikes that lag by <250 μs) is not consistent with the temporal dynamics of MC synchrony previously recorded in OB slices and anesthetized animals that show correlogram peak width of ~10 ms (Galán et al., 2006; Kashiwadani et al., 1999; Schoppa, 2006). Current OB network theory postulates that synchrony between MCs could occur as the result of interaction with the large inhibitory granule cell network (Mori et al., 1999). Consistent with theory, OB slice and anesthetized animal work has shown that granule cells can induce synchrony with ~10 ms temporal dynamics within distances as far as 500 μm (Galán et al., 2006; Kashiwadani et al., 1999; Schoppa, 2006). However, Figure 6 illustrates that the submillisecond synchrony observed in awake and behaving animals does not decay with distance even between SMCs recorded up to 1.5 mm apart.

Our observations raise the question of whether the synchrony measured between SMCs in awake, behaving animals is the exclusive result of the bulb's inhibitory interneuron network. In fact to our knowledge, the only examples of submillisecond synchrony that have been observed in other systems occurred when excitatory output from a single neuron diverged onto multiple target neurons (Alonso et al., 1996) or when the cells were coupled electrotonically (Takahashi and Sakurai, 2009; Wang et al., 2010). Because most synchronized SMCs are located many microns apart, it is unlikely that precise synchronization is caused by somatic gap junctions. MC lateral dendrite gap junctions could play a role, but if this were the case, ultrafast spike synchrony should be observed in the OB slices because in these slices, dendrodendritic circuits are intact.

We favor the view that our data showing precise synchronization is most likely due to coincident excitatory input to MCs through centrifugal input from anterior olfactory nucleus (AON) or OC (Matsutani, 2010; Restrepo et al., 2009). Cells responsible for centrifugal input from OC or AON would not be included in regular OB slices and are likely to be affected by anesthetics (e.g., urethane is thought to affect NMDA receptors; Daló and Larson, 1990), which explains why ultrafast synchronization is not found in these preparations. Interestingly, if excitatory centrifugal input is involved, then these fibers would have to make excitatory synapses on MCs. Such synapses have not been demonstrated, but Cajal suggested that they occur (Ramón y Cajal, 1904), and recent studies by Matsutani (2010) provide support for synaptic boutons from centrifugal fibers in the MC layer; future studies are required to resolve this issue. Importantly, Figure 6 shows that whereas SMC synchronization does not decrease as a function of distance, the differential response of synchronized spike trains to the rewarded and unrewarded odors is steeply dependent on distance, disappearing for distances >1.5 mm (Figure 6A, blue circles). The two circuits of limited spatial extent that could be involved in regulating divergent odorant responses in synchronized firing by MCs would be either the extensive MC lateral dendrite/granule cell circuit (Shepherd et al., 2004) or the interactions through short axon cells extending long axons that reach subsets of glomeruli (Kiyokage et al., 2010).

NA modulation is involved in the association of stimulus and reward in what has been called a "network reset" that takes place when the occurrence of task-relevant stimuli cannot be predicted and when the animal must learn a new association (Bouret and Sara, 2005). Indeed, neurons in the locus coeruleus that release NA in the OB are known to respond in rewarded trials during the go-no go task (Bouret and Sara, 2004, 2005). In addition, NA modulation of the OB circuit is known to be necessary to ensure odor discrimination for closely related odors in the go-no go task (Doucette et al., 2007). Our data suggest that part of this learning in the odor discrimination task involves developing large differential responses of synchronized firing trains from presumed MCs to the rewarded and unrewarded odors (Figure 7). The cellular mechanisms underlying this development of synchrony are not currently understood, but could involve an alteration of transmitter release (Pandipati et al., 2010).

If the SMCs we record from carry information on odor value as opposed to odor identity, a question that arises is how odor identity information is passed to higher-order centers. Tufted cells, a cell type that we did not target in the current study, are more abundant than MCs (Shepherd et al., 2004), and could carry information on odor identity. Middle tufted cells respond to odors and local processing of the odorant signal in the middle tufted cells differs from that in MCs (Griff et al., 2008; Nagayama et al., 2004). In addition, external tufted cells whose cell bodies lie adjacent to glomeruli could transmit information on odor identity (Wachowiak and Shipley, 2006), although whether these cells can carry information to higher-order centers has not been fully explored (Schoenfeld and Macrides, 1984; Schoenfeld et al., 1985). It is also possible that different subsets of MCs engage different networks in the piriform cortex. Indeed, in a previous publication we showed that a small percent (~2%) of the odor-divergent MCs did not change the z-score throughout a discrimination session or when odors changed between the rewarded and unrewarded state (Doucette and Restrepo, 2008). Thus, it is possible that a subset of MCs does carry information on odor identity, and the odor responsiveness of MCs within this subset may be minimally affected by behavioral context. Finally, our findings do not exclude the possibility that the same MCs that carry information on odor value also carry information on odor identity through another coding mechanism in either a simultaneous or sequential fashion, as found in taste cortical neurons (Miller and Katz, 2010). Indeed, regarding sequential transfer of information, it is known that SMCs respond differentially to odors within the first sniff after odor exposure (Cury and Uchida, 2010). These issues deserve future studies.

In summary, we find that SMCs separated by large distances (of up to 1.5 mm) and therefore innervating different glomeruli fire synchronously, and that synchronized firing conveys information on odor value, not odor identity. This is particularly relevant because the output from MCs innervating different glomeruli converges on OC pyramidal cells (Apicella et al., 2010), and synchronized firing of MCs is effective at eliciting excitation of OC pyramidal cells (Franks and Isaacson, 2006; Luna and Schoppa, 2008). Thus, our findings suggest that the circuit encompassing the MCs and the OC pyramidal cells is involved in evaluating information on odor value.

EXPERIMENTAL PROCEDURES

Microarray Implantation

Eight 8- to 10-week-old animals were implanted bilaterally with 2 × 4 electrode arrays (Figure 1A). Animals were anesthetized with an intraperitoneal ketamine-xylazine injection (composed of 100 μg/g and 20 μg/g, respectively). The electrode arrays were manufactured by Micro Probes Inc., composed of platinum iridium wire etched to a 2 μm tip, and coated with parylene C (3–4 MΩ at 1 kHz). The arrays were organized in a 2 × 4 pattern with 200 μm spacing with lengths of 4.2 to 4.8 mm angled at 45° along the long axis to ensure targeting to the MC layer (Figure 1A).

In this study, as reported previously by Kay and Laurent (1999) and Rinberg et al. (2006), no spikes were detected while the electrodes traversed the granule cell layer. Once the electrode reached the ventral MC, layer spikes with amplitudes ranging from 100 to 2000 μV were detected with spontaneous firing frequency characteristic of MCs (Figures S1A and S5, MCL). As shown in Figure S5, recording from the granule cell layer yielded significantly smaller voltage deviations. Recordings from electrodes displaying only such small voltage deviations were infrequent and were not analyzed to avoid contamination by granule-cell generated multiunit activity. Because granule cell signals were too small to be detected when thresholding based upon recordings in the MC layer, these cells almost certainly do not contribute to the multiunit activity detected in the MC layer. Once the MC layer was reached, the arrays were fixed in place with titanium skull screws and nail acrylic with one of the titanium screws serving as the ground. Although the electrodes do not record spikes from the granule cells, we term the recorded units "suspected MCs" because our measurements may include some internal tufted cells. All animal procedures were performed under a protocol approved by the institutional animal care and use committee of the University of Colorado Anschutz Medical Campus.

Surgery for Implantation of Sniff Cannulae

Surgical procedures for cannula implantation were based upon the work of Wesson et al. (2008). Briefly, animals were anesthetized as described above, and lidocaine was injected into the epidermis above the frontal nasal bone as a local anesthetic. An incision was made down the midline and the skull was cleaned with 3% H_20_2. Next, a hole was drilled 1 mm anterior to the frontal/nasal fissure and 1 mm lateral from the midline. A hollow cannula was then lowered into the hole and fixed in place with nail acrylic.

Imaging of the OBs Using MRI

Mice were anesthetized with nembutal (100 mg/kg) and perfused with 4% paraformaldehyde. Fixed heads were placed in PBS containing 5% Prohance (Bracco Diagnostics Inc, Princeton, NJ) and1% distilled H_2O for 2 weeks prior to imaging. Imaging experiments were conducted on a Bruker Biospec 7-T horizontal-bore system (Bruker Inc, Billerica, MA) controlled with Paravision 4.0 software. The brain specimens were placed inside a sealed container filled with Fomblin liquid (Solvay Slexis, West Deptford, NJ) to minimize artifacts arising from air-tissue interface. A standard 3D Fast Spin Echo sequence was used to acquire the 256 images for each head (repetition time, 500 ms; echo time, 8.6 ms; echo train length, 4; number of averages, 4; scan time, 11 hr 22 min). The imaging resolution was 78 μm isotropic. Volumes were constructed using ImageJ 1.42q software and final images were contrast enhanced using Photoshop 6.0.

Initial Training in the Go-No Go Task

The mice were trained using water reinforcement and underwent testing in go-no go trials (Figures 1Bi and 1C) (Doucette et al., 2007; Doucette and Restrepo, 2008; Slotnick and Restrepo, 2005). All mice were first trained to distinguish 1% isoamyl acetate versus 1% cumin aldehyde (v/v in mineral oil). The animal's performance was evaluated in blocks of 20 trials (10 rewarded and 10 unrewarded, presented at random). Each block's percent correct value represents the percent of trials in which the odors were correctly discriminated and associated with the appropriate behavioral action. Each session included 6–10 blocks of 20 trials. Once the animals learned to discriminate between isoamyl acetate and cumin aldehyde, they were ready for the novel odor discrimination task described below.

Screening for Responsive Novel Odor Pairs

As described in the Supplemental Text, we screened novel odors that presumably would stimulate glomeruli in the ventral surface of the OB (the electrodes were targeted to this area of the bulb). Choice of odors is described in the Supplemental Text. In order to screen these odors in a behaviorally neutral setting, an 8 × 8 × 13 cm chamber was constructed wherein the mouse was exposed passively to odors. Odors were introduced on a constant background odor stream for 2 s with an intertrial interval of 60 s. Odors were screened in groups of 12 or 15 per session. After a session the data were analyzed overnight and the best two odors (odors A and B) were used in the subsequent odor discrimination task. The odors shown in italics in Table S1 were found to elicit responses more often than the others.

Once we identified responsive novel odors A and B, we proceeded the next day with a novel odor pair discrimination task. As in previous studies, in order to make the odor discrimination task difficult, we asked mice to discriminate between odor mixtures (Doucette et al., 2007; Doucette and Restrepo, 2008). Odor mixtures have been employed in several studies of the speed of olfactory processing (Abraham et al., 2004; Uchida and Mainen, 2003) and odor similarity determinations (Doucette et al., 2007; Kay et al., 2006). In our behavioral paradigm the animals learned to discriminate between odor A and a 1:1 mixture of odor A:odor B at an overall concentration of 1% by volume in mineral oil. Measurements using a photoionization detector indicated that odors arrived at the chamber at ~0.3 s after routing of the odor into the port (mini-PID; Aurora Scientific Inc., Aurora, ON, Canada).

Delivery of Adrenergic Receptor Antagonists into the OB

Six animals were implanted bilaterally with multielectrode arrays containing a central cannula for adrenergic drug delivery. Multielectrode arrays with cannulae were constructed in a similar 2 × 4 pattern as described above with the addition of a 23G stainless steel tube in the center of the array terminating 2 mm above the electrode tips so that it would sit above the bulb while the electrodes were implanted within the bulb as described above.

For adrenergic drug delivery we used the same procedure as in a previous publication (Doucette et al., 2007). Briefly, immediately prior to behavioral testing, animals received bilateral injection of a test solution under isoflourane anesthesia. The infusions consisted of bilateral 2 μl injections of the desired drug(s) dissolved in HEPES-buffered saline over 10 min. We took advantage of the fact that there are well characterized subtype-specific adrenergic antagonists with known specificity for the different receptor subtypes (Pupo and Minneman, 2001) and that addition of a mixture of β and α adrenergic inhibitors affects discrimination of closely related odors in our go-no go task (Doucette et al., 2007). As in our previous study, we used a mixture of alprenolol (general β blocker, 28 nmols) and phentolamine (general α blocker, 28 nmols). Five minutes following drug delivery, the injection needle was replaced with the cannula-sealing stylet. Animals then required 5–10 min to recover fully from isoflourane anesthesia. In our previous study we showed that this procedure resulted in drug infusion that was limited to the OB (Doucette et al., 2007).

Monitoring Sniffing

We monitored sniffing by recording intranasal pressure via implanted nasal cannulae connected to a pressure sensor (Model No. 24PCEFA6G(EA), 0–0.5 psi, Honeywell, Canada) via polyethylene tubing. The sensor was mounted on a commutator (TDT: Tucker Davis Technologies, Alachua, FL) to allow for the animal's free rotation during the task. Pressure transients were digitized and sampled at 24 kHz. Sniff data was analyzed for instantaneous frequency as in Wesson et al. (2008).

Recording Setup

The output of the two electrode arrays was directed to a 16 channel TDT 1× gain headstage connected to a TDT motorized commutator that was in turn connected to a CWE 16 channel amplifier and band-pass filter (CWE, Ardmore, PA). The signal from 14 electrodes was amplified 2000 times and filtered at 300–3000 Hz before outputting to a Data Translation Inc. (Marlboro, MA) DT3010 A/D card in a PC. Data were acquired at 24 kHz with custom software written in MATLAB (MathWorks, Inc., Natick, MA). Digitized behavioral events from the Slotnick olfactometer (licks, nose pokes, and odor on) were also acquired in real time.

Offline Spike Clustering

Offline spike clustering was performed as in a previous publication (Doucette and Restrepo, 2008). Briefly, custom software written in MATLAB was used to threshold each channel at 3× root mean squared (RMS) of the baseline noise. Every thresholded spike (24 points at 24 kHz) was saved from each channel and imported into a second program where we clustered the waveforms of similar shape by performing wavelet decomposition and superparamagnetic clustering using the method and MATLAB software developed by Quiroga et al. (2004). In addition to determining 18 wavelet coefficients used in the Quiroga program, our modified program also determined the first three coefficients of a PC analysis of the spikes and calculated the peak to valley ratio. As explained in Quiroga et al. (2004), the program then proceeded to determine which of these descriptors showed a multimodal distribution and used the ten best descriptors to separate the spikes into well-defined clusters using superparamagnetic clustering. We defined a single unit using the criterion of finding <3% of the spikes in the refractory period of 2 ms in the interspike interval (ISI) histogram. On average, we obtained 12 multiunits and 5 single units per experiment. We examined the stability of the classification method over time to ensure that single units were not misclassified. Spikes that occurred in every channel at 3–8 Hz when the animal was licking (likely an electrical event elicited by licking) were easily identified and excluded from the analysis.

Analysis of Synchronized Spikes

In a preliminary survey of correlograms such as those shown in Figure 2, we found a large number of pairs of single units and multiunits that exhibited peaks different from correlograms calculated after the original spike trains had been shuffled by a random time ranging between plus or minus one mean ISI (ISI shuffle, red lines in Figures 2B1–2B3). In order to tally the number of unit pairs that exhibited significant synchronized firing, we wrote a MATLAB program that tested, for all trials in a session in the RA (0.5 to 2.5 s), whether the number of synchronized spikes, defined as spikes in the two units that were within 250 μs of each other, was significantly different in a t test from the number of synchronized spikes after ISI shuffling. The choice of the 250 μs window was not arbitrary. We performed a thorough survey of the data by surveying cross correlograms such as those shown in Figures 2B1–2B3, and we found a robust cross correlation different from that of the shuffled spike trains that fell within the 250 μs lag window. The p value for the t test was corrected for multiple comparisons within each session using an FDR method (Curran-Everett, 2000). For those unit pairs that exhibited significant synchronization, a synchronized spike train was generated that included all spikes in the first (reference) unit that were within 250 μs of the second (partner) unit.

Data Analysis

Analysis was performed using custom written MATLAB programs tested using simulated data (see Figure S6). A t test was used to classify unit firing rates or synchronized spike train firing rates as odor "divergent" when the responses to the rewarded and unrewarded odors were statistically different. Within each block of 20 trials, differences between firing rates in response to the different odors (ten rewarded and ten unrewarded odor trials) in the odor RA (0.5 to 2.5 s) were assessed using the t test. Within each experiment, the calculated p values were corrected for multiple comparisons using the FDR method (Curran-Everett, 2000). In our previous publication (Doucette and Restrepo, 2008), we had found that occasionally, a single block was significantly different between rewarded and unrewarded trials in the reference interval. Accordingly, we adopted the conservative measure of classifying a unit as divergent only when the p value for the t test of significant differences was below the FDR-corrected p value in two or more blocks. As a control, differences in firing rate between rewarded and unrewarded trials in the same block were compared using the same procedure in the interval from −1.5 to 0.5 s in the absence of odor (the prestimulus interval) to assess the effectiveness of the correction for multiple comparisons. Odors did not elicit divergent responses in this control time range (data not shown).

At test was also used to classify units as "responsive." The rate of firing in the RA (0.5 to 2.5 s) was compared with the firing rate during the reference interval (−1.5 to 0.5 s). The FDR was used to correct for multiple comparisons,

and a unit was classified as responsive only if p values fell below FDR in at least two or more blocks.

SUPPLEMENTAL INFORMATION

Supplemental Information for this article includes six figures, one table, a Supplemental Discussion, and Supplemental Experimental Procedures and can be found with this article online at doi:10.1016/j.neuron.2011.02.024.

ACKNOWLEDGMENTS

We would like to thank Drs. Gidon Felsen, Nathan Schoppa, and Dan Tollin for discussions; Dr. Ed Hsu; Osama Abdulla; and the University of Utah Small Animal MRI Facility. This work was funded by NIH grants DC00566 (D.R.), DC04657 (D.R.), DC008855 (D.R.), DC008066 (W.D.), and DC002994 (M.L.).

Accepted: January 12, 2011
Published: March 23, 2011

REFERENCES

Abraham, N.M., Spors, H., Carleton, A., Margrie, T.W., Kuner, T., and Schaefer, A.T. (2004). Maintaining accuracy at the expense of speed: Stimulus similarity defines odor discrimination time in mice. Neuron *44*, 865–876.

Alonso, J.M., Usrey, W.M., and Reid, R.C. (1996). Precisely correlated firing in cells of the lateral geniculate nucleus. Nature *383*, 815–819.

Apicella, A., Yuan, Q., Scanziani, M., and Isaacson, J.S. (2010). Pyramidal cells in piriform cortex receive convergent input from distinct olfactory bulb glomeruli. J. Neurosci. *30*, 14255–14260.

Aungst, J.L., Heyward, P.M., Puche, A.C., Karnup, S.V., Hayar, A., Szabo, G., and Shipley, M.T. (2003). Centre-surround inhibition among olfactory bulb glomeruli. Nature *426*, 623–629.

Bailey, C.H., and Kandel, E.R. (2008). Synaptic remodeling, synaptic growth and the storage of long-term memory in Aplysia. Prog. Brain Res. *169*, 179–198.

Bouret, S., and Sara, S.J. (2004). Reward expectation, orientation of attention and locus coeruleus-medial frontal cortex interplay during learning. Eur. J. Neurosci. *20*, 791–802.

Bouret, S., and Sara, S.J. (2005). Network reset: A simplified overarching theory of locus coeruleus noradrenaline function. Trends Neurosci. *28*, 574–582.

Chang, F.C., and Scott, T.R. (1984). Conditioned taste aversions modify neural responses in the rat nucleus tractus solitarius. J. Neurosci. *4*, 1850–1862.

Curran-Everett, D. (2000). Multiple comparisons: Philosophies and illustrations. Am. J. Physiol. Regul. Integr. Comp. Physiol. *279*, R1–R8.

Cury, K.M., and Uchida, N. (2010). Robust odor coding via inhalation-coupled transient activity in the mammalian olfactory bulb. Neuron *68*, 570–585.

Daló, N.L., and Larson, A.A. (1990). Effects of urethane and ketamine on substance P- and excitatory amino acid-induced behavior in mice. Eur. J. Pharmacol. *184*, 173–177.

Doucette, W., and Restrepo, D. (2008). Profound context-dependent plasticity of mitral cell responses in olfactory bulb. PLoS Biol. *6*, e258.

Doucette, W., Milder, J., and Restrepo, D. (2007). Adrenergic modulation of olfactory bulb circuitry affects odor discrimination. Learn. Mem. *14*, 539–547.

Egaña, J.I., Aylwin, M.L., and Maldonado, P.E. (2005). Odor response properties of neighboring mitral/tufted cells in the rat olfactory bulb. Neuroscience *134*, 1069–1080.

Franks, K.M., and Isaacson, J.S. (2006). Strong single-fiber sensory inputs to olfactory cortex: Implications for olfactory coding. Neuron *49*, 357–363.

Friedrich, R.W., Habermann, C.J., and Laurent, G. (2004). Multiplexing using synchrony in the zebrafish olfactory bulb. Nat. Neurosci. *7*, 862–871.

Galán, R.F., Fourcaud-Trocmé, N., Ermentrout, G.B., and Urban, N.N. (2006). Correlation-induced synchronization of oscillations in olfactory bulb neurons. J. Neurosci. *26*, 3646–3655.

Gao, Y., and Strowbridge, B.W. (2009). Long-term plasticity of excitatory inputs to granule cells in the rat olfactory bulb. Nat. Neurosci. *12*, 731–733.

Gire, D.H., and Schoppa, N.E. (2008). Long-term enhancement of synchronized oscillations by adrenergic receptor activation in the olfactory bulb. J. Neurophysiol. *99*, 2021–2025.

Gold, J.I., and Shadlen, M.N. (2007). The neural basis of decision making. Annu. Rev. Neurosci. *30*, 535–574.

Gray, C.M., Freeman, W.J., and Skinner, J.E. (1986). Chemical dependencies of learning in the rabbit olfactory bulb: Acquisition of the transient spatial pattern change depends on norepinephrine. Behav. Neurosci. *100*, 585–596.

Griff, E.R., Mafhouz, M., and Chaput, M.A. (2008). Comparison of identified mitral and tufted cells in freely breathing rats: II. Odor-evoked responses. Chem. Senses *33*, 793–802.

Kashiwadani, H., Sasaki, Y.F., Uchida, N., and Mori, K. (1999). Synchronized oscillatory discharges of mitral/tufted cells with different molecular receptive ranges in the rabbit olfactory bulb. J. Neurophysiol. *82*, 1786–1792.

Kay, L.M., and Beshel, J. (2010). A beta oscillation network in the rat olfactory system during a 2-alternative choice odor discrimination task. J. Neurophysiol. *104*, 829–839.

Kay, L.M., and Laurent, G. (1999). Odor- and context-dependent modulation of mitral cell activity in behaving rats. Nat. Neurosci. *2*, 1003–1009.

Kay, L.M., Krysiak, M., Barlas, L., and Edgerton, G.B. (2006). Grading odor similarities in a Go/No-Go task. Physiol. Behav. *88*, 339–346.

Kiyokage, E., Pan, Y.Z., Shao, Z., Kobayashi, K., Szabo, G., Yanagawa, Y., Obata, K., Okano, H., Toida, K., Puche, A.C., and Shipley, M.T. (2010). Molecular identity of periglomerular and short axon cells. J. Neurosci. *30*, 1185–1196.

Komura, Y., Tamura, R., Uwano, T., Nishijo, H., Kaga, K., and Ono, T. (2001). Retrospective and prospective coding for predicted reward in the sensory thalamus. Nature *412*, 546–549.

Luna, V.M., and Schoppa, N.E. (2008). GABAergic circuits control input-spike coupling in the piriform cortex. J. Neurosci. *28*, 8851–8859.

Mandairon, N., and Linster, C. (2009). Odor perception and olfactory bulb plasticity in adult mammals. J. Neurophysiol. *101*, 2204–2209.

Martin, C., Gervais, R., Messaoudi, B., and Ravel, N. (2006). Learning-induced oscillatory activities correlated to odour recognition: A network activity. Eur. J. Neurosci. *23*, 1801–1810.

Matsutani, S. (2010). Trajectory and terminal distribution of single centrifugal axons from olfactory cortical areas in the rat olfactory bulb. Neuroscience *169*, 436–448.

Miller, P., and Katz, D.B. (2010). Stochastic transitions between neural states in taste processing and decision-making. J. Neurosci. *30*, 2559–2570.

Mori, K., Nagao, H., and Yoshihara, Y. (1999). The olfactory bulb: Coding and processing of odor molecule information. Science *286*, 711–715.

Nagayama, S., Takahashi, Y.K., Yoshihara, Y., and Mori, K. (2004). Mitral and tufted cells differ in the decoding manner of odor maps in the rat olfactory bulb. J. Neurophysiol. *91*, 2532–2540.

Nissant, A., Bardy, C., Katagiri, H., Murray, K., and Lledo, P.M. (2009). Adult neurogenesis promotes synaptic plasticity in the olfactory bulb. Nat. Neurosci. *12*, 728–730.

Pandipati, S., Gire, D.H., and Schoppa, N.E. (2010). Adrenergic receptor-mediated disinhibition of mitral cells triggers long-term enhancement of synchronized oscillations in the olfactory bulb. J. Neurophysiol. *104*, 665–674.

Pantoja, J., Ribeiro, S., Wiest, M., Soares, E., Gervasoni, D., Lemos, N.A., and Nicolelis, M.A. (2007). Neuronal activity in the primary somatosensory thalamocortical loop is modulated by reward contingency during tactile discrimination. J. Neurosci. *27*, 10608–10620.

Pupo, A.S., and Minneman, K.P. (2001). Adrenergic pharmacology: Focus on the central nervous system. CNS Spectr. *6*, 656–662.

Quiroga, R.Q., Nadasdy, Z., and Ben-Shaul, Y. (2004). Unsupervised spike detection and sorting with wavelets and superparamagnetic clustering. Neural Comput. *16*, 1661–1687.

Ramón y Cajal, S. (1904). Textura del Sistema Nervioso del Hombre y de los Vertebrados (Madrid: Moya).

Restrepo, D., Doucette, W., Whitesell, J.D., McTavish, T.S., and Salcedo, E. (2009). From the top down: Flexible reading of a fragmented odor map. Trends Neurosci. *32*, 525–531.

Rinberg, D., Koulakov, A., and Gelperin, A. (2006). Sparse odor coding in awake behaving mice. J. Neurosci. *26*, 8857–8865.

Roberts, A.C., and Glanzman, D.L. (2003). Learning in Aplysia: Looking at synaptic plasticity from both sides. Trends Neurosci. *26*, 662–670.

Schoenfeld, T.A., and Macrides, F. (1984). Topographic organization of connections between the main olfactory bulb and pars externa of the anterior olfactory nucleus in the hamster. J. Comp. Neurol. *227*, 121–135.

Schoenfeld, T.A., Marchand, J.E., and Macrides, F. (1985). Topographic organization of tufted cell axonal projections in the hamster main olfactory bulb: An intrabulbar associational system. J. Comp. Neurol. *235*, 503–518.

Schoppa, N.E. (2006). Synchronization of olfactory bulb mitral cells by precisely timed inhibitory inputs. Neuron *49*, 271–283.

Shepherd, G.M., Chen, W.R., and Greer, C.A. (2004). Olfactory bulb. In The Synaptic Organization of the Brain, G.M. Shepherd, ed. (New York: Oxford University Press), pp. 159–204.

Shuler, M.G., and Bear, M.F. (2006). Reward timing in the primary visual cortex. Science *311*, 1606–1609.

Slotnick, B.M., and Restrepo, D. (2005). Olfactometry with mice. In Current Protocols in Neuroscience, J.N. Crawley, C.R. Gerefen, M.A. Rogawski, D.R. Sibley, P. Skolnick, and S. Wray, eds. (New York: John Wiley and Sons, Inc), pp. 1–24.

Stopfer, M., Bhagavan, S., Smith, B.H., and Laurent, G. (1997). Impaired odour discrimination on desynchronization of odour-encoding neural assemblies. Nature *390*, 70–74.

Takahashi, S., and Sakurai, Y. (2009). Sub-Millisecond Firing Synchrony of Closely Neighboring Pyramidal Neurons in Hippocampal CA1 of Rats During Delayed Non-Matching to Sample Task. Front Neural Circuits *3*, 9.

Tan, J., Savigner, A., Ma, M., and Luo, M. (2010). Odor information processing by the olfactory bulb analyzed in gene-targeted mice. Neuron *65*, 912–926.

Uchida, N., and Mainen, Z.F. (2003). Speed and accuracy of olfactory discrimination in the rat. Nat. Neurosci. *6*, 1224–1229.

Wachowiak, M., and Shipley, M.T. (2006). Coding and synaptic processing of sensory information in the glomerular layer of the olfactory bulb. Semin. Cell Dev. Biol. *17*, 411–423.

Wallis, J.D., and Kennerley, S.W. (2010). Heterogeneous reward signals in prefrontal cortex. Curr. Opin. Neurobiol. *20*, 191–198.

Wang, Y., Barakat, A., and Zhou, H. (2010). Electrotonic coupling between pyramidal neurons in the neocortex. PLoS ONE *5*, e10253.

Wesson, D.W., Donahou, T.N., Johnson, M.O., and Wachowiak, M. (2008). Sniffing behavior of mice during performance in odor-guided tasks. Chem. Senses *33*, 581–596.

Wilson, D.A., and Leon, M. (1988). Spatial patterns of olfactory bulb single-unit responses to learned olfactory cues in young rats. J. Neurophysiol. *59*, 1770–1782.

Wilson, R.I., and Mainen, Z.F. (2006). Early events in olfactory processing. Annu. Rev. Neurosci. *29*, 163–201.